



# Extraction of copper, zinc and cadmium from copper–cadmium-bearing slag by oxidative acid leaching process

Meng Li, Ying Zhang, Xiao-Hui Wang, Jian-Guang Yang, Shan Qiao, Shi-Li Zheng\* , Yi Zhang

Received: 20 May 2015/Revised: 28 May 2015/Accepted: 9 May 2016/Published online: 23 June 2016  
© The Nonferrous Metals Society of China and Springer-Verlag Berlin Heidelberg 2016

**Abstract** An intensified oxidative acid leaching of copper–cadmium-bearing slag featuring using high-efficient oxygen carrier, such as activated carbon, was investigated to achieve high leaching rate of valuable metals. The effects of leaching variables, including agitation rate, sulfuric acid concentration, temperature, slag particle size, activated carbon and cupric ion concentration, were examined. It is found that leaching rates of cadmium and zinc both exceed 99 % in a very short time, but for copper, leaching rate of 99 % is achieved under the optimized leaching parameters, which are agitation rate of 100 r·min<sup>-1</sup>, sulfuric acid concentration of 15 wt%, leaching temperature of 80 °C, slag particle size of 48–75 μm, activated carbon concentration of 3 g·L<sup>-1</sup>, liquid-to-solid ratio of 4:1, oxygen flow rate of 0.16 L·min<sup>-1</sup>, and leaching time of 60 min. The macro-leaching kinetics of copper metal was analyzed, and it is concluded that the inner diffusion is the controlling step, with apparent activation energy of 18.6 kJ·mol<sup>-1</sup>. The leaching solution with pH value of 2–4 can be designed to selectively extract valuable metals without neutralization, and the leaching residue can be treated by prevailing Pb smelting process.

**Keywords** Copper–cadmium-bearing slag; Catalytic oxidative acid leaching; Activated carbon; Kinetics

## 1 Introduction

Zinc is the third most common nonferrous metal after aluminum and copper, which has wide application in the areas of plating, coating and alloying [1–3]. Currently, 80 %–85 % zinc is produced from zinc sulfide concentrates by the hydrometallurgical methods of roasting-acid leaching-purifying-electrowinning process or oxygen pressure acid leaching-purifying-electrowinning process worldwide [4]. Copper and cadmium are the main associated valuable metals in zinc resources and can be leached out in company with zinc, which have to be removed to avoid their influence on subsequent zinc electrolysis. According to the standard electrode potentials, these cations can be reduced with zinc powder to form corresponding metals and be removed from the solution. Thus, during the purification unit, large quantities of copper–cadmium-bearing slags were generated. Through rough calculation, more than half million tons of this slag was produced per year in China. And most of the residue was not used efficiently. This residue not only takes massive land, but also comes forth great risk of environmental pollution, as it contains significant content of lead, as well as some arsenic, cadmium, and such toxic ingredients have the potential of being dissolved by rain water [5, 6].

Different routes of metal recovery from copper–cadmium-bearing slag have been tried for decades, which primarily include acid leaching-purifying-reducing-electrowinning process and acid leaching-purifying-extracting-stripping process [7]. The leaching procedure of the two methods is very similar, and the main difference between

---

M. Li  
School of Metallurgy, Northeastern University,  
Shenyang 110819, China

M. Li, Y. Zhang, X.-H. Wang, S. Qiao, S.-L. Zheng\*, Y. Zhang  
National Engineering Laboratory for Hydrometallurgical  
Cleaner Production Technology, Key Laboratory of Green  
Process and Engineering, Institute of Process Engineering,  
Chinese Academy of Sciences, Beijing 100190, China  
e-mail: slzheng@ipe.ac.cn

J.-G. Yang  
School of Metallurgy and Environment, Central South  
University, Changsha 410083, China

them is the treatment of the leaching solution after purification. Reducing-electrowinning process and extracting-stripping process are very simple to implement and easy to operate, but the leaching procedure of the two routes has the problem of complex technical processes and low leaching rate [7]. So many researchers consider the leaching unit is the limiting stage of the whole route. Nowadays, most of the factories choose to extract zinc and cadmium first before subsequent copper extraction in the leaching section. Nonetheless, the two-stage leaching process is not economically feasible due to the setup of extra facilities to store solution and residue [8]. Usually, manganese dioxide (or pyrolusite) or hydrogen peroxide is used by many plants as oxidant during the oxidative sulfuric acid leaching; however, the former will introduce impurities and the latter is too expensive. So it is necessary to choose a more suitable oxidant in the oxidative sulfuric acid leaching step. Oxygen is known as a cheap and clean oxidant, and has been widely used in many applications. In this regard, oxidative sulfuric acid leaching of copper–cadmium-bearing slag by using oxygen has been proposed.

Further, in order to improve the oxygen transfer efficiency, the catalytic effect of activated carbon has also been examined. Activated carbon is a type of porous material with large surface areas and has been widely used as adsorbent, catalyst, and catalyst carrier [9, 10]. And there are many unsaturated oxygenated functional groups associated with the porous structure, including carboxyl, carboxyl anhydride, carbonyl, lactone, phenolic, ether, pyrone, chromene, etc. These functional groups were reported to exhibit catalytic behaviors in many chemical reactions, drawing much research attention [11–14]. However, activated carbon-assisted oxidative sulfuric acid leaching of copper–cadmium-bearing slag has rarely been reported.

In this work, a method featuring catalytic-assisted oxidative acid leaching of copper–cadmium-bearing slag was studied. Key operation parameters including agitation speed, sulfuric acid concentration, temperature, slag particle size, catalyst (activated carbon and cupric ions) concentration were systematically examined. Furthermore, the macro-kinetic parameters were assessed using shrinking core model, and then the rate controlling step for copper metal leaching was determined. Finally, the possible handling strategies of the leachate and leaching residue were suggested.

## 2 Experimental

### 2.1 Materials

The slag used in this research was supplied by Hunan Shuikoushan Nonferrous Metals Group Co., Ltd, which was dried for 12 h at 110 °C before crushed and screened

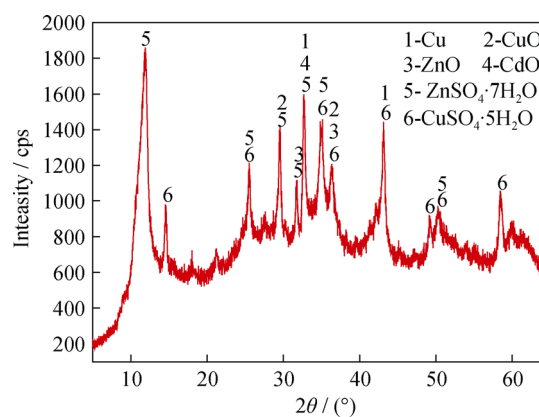


**Fig. 1** XRD pattern of copper–cadmium-bearing slag

to obtain slag with different sizes. Phase compositions were determined by X-ray diffraction (XRD) analysis, as shown in Fig. 1. Theoretically speaking, the main phases in the copper–cadmium-bearing slag should be Cu metal, Cd metal and excess zinc metal; however, owing to the oxidation effect of air and the corrosion of surface-adhered sulfuric acid solution, the phases from Fig. 1 are Cu, CuO, CdO, ZnO, ZnSO<sub>4</sub>·7H<sub>2</sub>O and CuSO<sub>4</sub>·5H<sub>2</sub>O. The chemical compositions of the slag determined by inductively coupled plasma atomic emission spectrometry (ICP-AES) are presented in Table 1, from which it could be noted that the main elements are Zn, Cd and Cu.

Sulfuric acid used in this research was obtained from Beijing Chemical Works with reagent grade (96 %–98 %). Activated carbon was supplied by Green-Source (China). Oxidant of compressed oxygen was bought from Beijing Chemical Works with industrial grade. Water was purified with Milli-Q (Millipore Corp.) equipment before use.

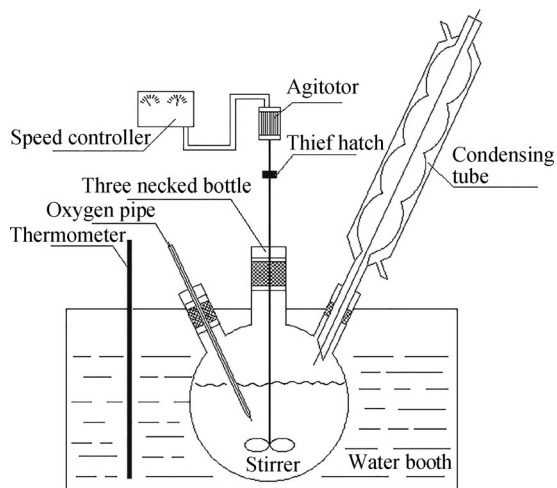
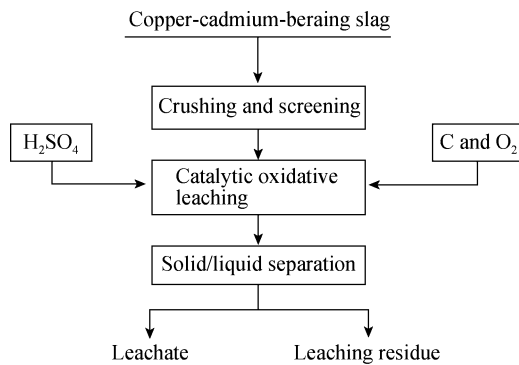
### 2.2 Experimental setup and procedure

The experimental setup is shown in Fig. 2, and the process flow sheet is presented in Fig. 3. For one batch of experiment, certain amount of slag, generally 100 g, was dispersed by approximately 400 ml high-purity water in a three-neck flask (positioned in a water bath) with mechanical stirring (100–400 r·min<sup>-1</sup>). When the slurry was heated up to the pre-set temperature, certain amount of concentrated sulfuric acid was injected into the flask gently. And then compressed oxygen was flowed into the reactor controlled by a regulator. In some experiments, catalysts were mixed with the slurry as well. To investigate the leaching dynamics, several milliliters of slurry was sampled at a certain intervals (5–30 min) to analyze the leaching rates of different metals.

After leaching, the slurry was filtered. And the filter cake was washed twice with dilute H<sub>2</sub>SO<sub>4</sub> solution and

**Table 1** Chemical compositions of copper–cadmium-bearing slag (wt%)

Zn	Cd	Cu	Ca	Al	Mg	Pb
25.76	20.38	9.53	2.27	0.49	0.62	0.55

**Fig. 2** Experimental setup for oxidative sulfuric acid leaching**Fig. 3** General flow chart for sulfuric acid leaching of copper–cadmium-bearing slag

then deionized water, respectively, to avoid the hydrolysis of leached-out metals and remove free acid. Then the cake was dried at 110 °C for 12 h, and its chemical and phase compositions were analyzed by inductively coupled plasma atomic emission spectrometer (ICP-AES, America, Pekin-Elmer) and X-ray diffractometer (XRD, Netherlands, PANalytical) equipped with Cu K $\alpha$  radiation, respectively. Meanwhile, the leachate was collected to analyze its acidity and chemical compositions, respectively, by pH meter and ICP-AES.

The metal leaching rates were calculated using Eq. (1). Owing to the undissolvable property of Pb during the

sulfuric acid leaching, Pb was used as the reference substance, and the mass content ratio change of concerned metal to lead was used as the evaluation parameter to calculate the leaching rate.

$$R = \frac{M_i/M_{Pb} - m_i/m_{Pb}}{M_i/M_{Pb}} \times 100\% \quad (1)$$

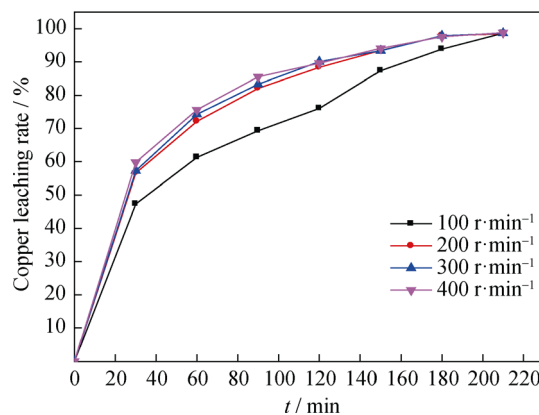
where  $R$  is the leaching rate of Cu, Cd or Zn;  $M_i$  and  $m_i$  are corresponding mass contents of concerned metal in the original copper–cadmium-bearing slag and in residue, respectively;  $M_{Pb}$  and  $m_{Pb}$  are mass contents of Pb in the original slag and in residue, respectively.

### 3 Results and discussion

#### 3.1 Effects of main leaching parameters

##### 3.1.1 Agitation speed

High stirring speed can reduce the thickness of diffusion layer effectively. In order to get meaningful data on leaching dynamics, high-enough agitation speed is very crucial to eliminate the external diffusion controlling. The relationship of copper leaching rate against leaching time under different stirring speeds is plotted in Fig. 4. It could be noted that even the speed increases dramatically from 100 to 400 r·min<sup>-1</sup>, totally neglectable effect is observed. They all reach the highest leaching rate of 99 % after 3 h. The reason that stirring speed shows no obvious effect is that the oxygen from the cylinder controlled by the regulator and flow meter is purged into the bottom of the reactor, and the rising bubbles have the function of agitation. The external diffusion effect can be eliminated even though 100 r·min<sup>-1</sup> is selected; hence, it is not the rate controlling step [15–19].

**Fig. 4** Effect of agitation speed on copper leaching rate (other leaching parameters: sulfuric acid concentration of 15 wt%, temperature of 80 °C, liquid-to-solid ratio of 4:1, particle size of 48–75  $\mu$ m, oxygen flow rate of 0.16 L·min<sup>-1</sup>)

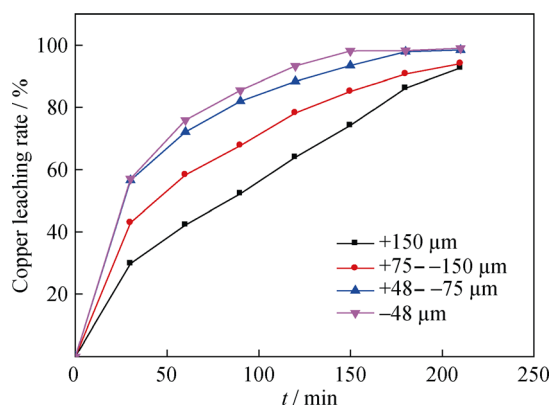


**Fig. 5** Effect of slag particle size on copper leaching rate (other leaching parameters: agitation rate of  $100 \text{ r}\cdot\text{min}^{-1}$ , sulfuric acid concentration of 15 wt%, temperature of  $80 \text{ }^\circ\text{C}$ , liquid-to-solid ratio of 4:1, oxygen flow rate of  $0.16 \text{ L}\cdot\text{min}^{-1}$ )

### 3.1.2 Slag particle size

The effect of slag particle size on Cu leaching rate is shown in Fig. 5. It is a general rule that a decrease in particle size will accelerate the reaction rate, owing to the increase of the contacting surface area among the reactants. The data in Fig. 5 clearly demonstrate that the leaching rates increase along with the decrease in particle size, and less significant effect is observed when the particle size is  $-75 \mu\text{m}$ . So, the particle size of slag could be controlled at  $48\text{--}75 \mu\text{m}$ .

### 3.1.3 Sulfuric acid concentration

The effect of sulfuric acid concentration on valuable metal leaching rates is shown in Fig. 6. Because a fixed liquid-to-solid ratio is chosen, a higher sulfuric acid concentration means a higher excess coefficient of sulfuric acid. According to the chemical composition of the slag, it can be calculated out that the stoichiometric acid concentration should be 16 wt% with the assumption that no sulfate salts exist. According to the standard electrode potentials, Zn and Cd metals are prone to dissolving in sulfuric acid solution easily, easier for their oxides. Thus, under the circumstance that the amount of sulfuric acid is theoretically enough, no effect can be seen on Zn and Cd leaching rates. As for Cu, much has been oxidized to its oxide state by air when piling, so 99 % copper can be dissolved with the assistance of oxygen. However, when sulfuric acid concentration is lower than its theoretical concentration, about 10 wt%, the Zn and Cd leaching rates still keep at a high value, much higher than that for copper, indicating that  $\text{H}^+$  capture ability of Zn and Cd is stronger than that of Cu. And, because small proportions of the metals are existed in their sulfate salt states, which will not consume sulfuric acid, the real stoichiometric sulfuric acid concentration should be lower than

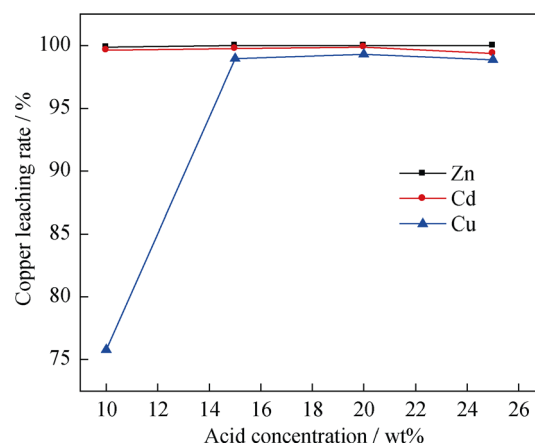


**Fig. 6** Effect of sulfuric acid concentration on copper leaching rate (other leaching parameters: agitation rate of  $100 \text{ r}\cdot\text{min}^{-1}$ , particle size of  $48\text{--}75 \mu\text{m}$ , temperature of  $80 \text{ }^\circ\text{C}$ , liquid-to-solid ratio of 4:1, oxygen flow rate of  $0.16 \text{ L}\cdot\text{min}^{-1}$ )

16 wt%. For these three metals, pretty high leaching rates of 99 % are achieved under initial sulfuric acid concentration of 15 wt%. Even though choosing a concentration of higher than 15 wt% can guarantee definitely high leaching rates, excessive acid will bring burden to the following separation procedures. Consequently, optimum sulfuric acid concentration should be 15 wt%.

### 3.1.4 Leaching temperature

The effect of leaching temperatures ranging from 40 to  $100 \text{ }^\circ\text{C}$  is assessed. The relationship of copper leaching rate versus leaching time at different temperatures is plotted in Fig. 7, showing that temperature affects Cu leaching rate significantly. The higher the temperature is, the faster the leaching rate is. Platforms appear after 3 h almost at all temperatures. It could be noted that a better temperature should be  $80 \text{ }^\circ\text{C}$ , which is concurred with the earlier literature reports [20–23].

It is unexpected that the copper leaching rate can reach a very high level in about 0.5 h, as shown in Fig. 7, which should be due to the presence of CuO phase in the original slag. In order to verify this, the leaching experiments were carried out in non-oxidative nitrogen atmosphere at different temperatures for 40 min, and the copper leaching rate curves versus leaching time are plotted in Fig. 8. The results indicate that the copper leaching rate can reach 63 % in about 30 min and keeps constant. Because Cu metal will not be dissolved under non-oxidative atmosphere, CuO contributes to the high leaching rate in the earlier stage. In order to calculate the Cu metal oxidative leaching dynamic parameters, the background brought by CuO was deducted, and the recalculated profiles are shown in Fig. 9, which will be used later for the dynamic analysis.

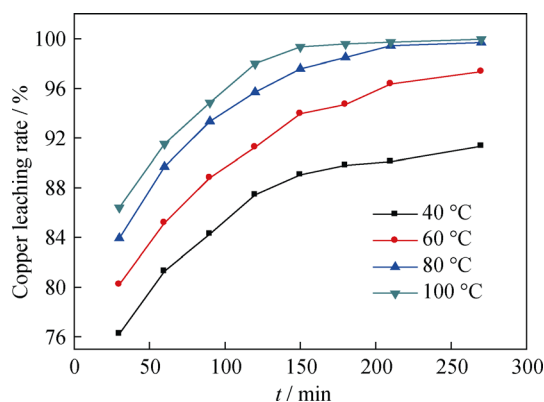


**Fig. 7** Effect of leaching temperatures on copper leaching rate when flowing oxygen (other leaching parameters: agitation rate of  $100 \text{ r}\cdot\text{min}^{-1}$ , particle size of  $48\text{--}75 \mu\text{m}$ , acid concentration of 15 wt%, liquid-to-solid ratio of 4:1, oxygen flow rate of  $0.16 \text{ L}\cdot\text{min}^{-1}$ )

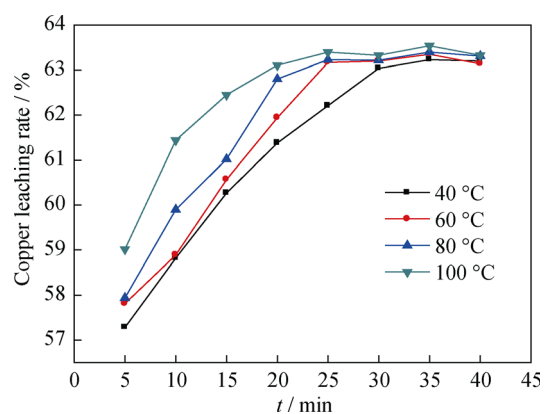


**Fig. 8** Effect of leaching temperatures on Copper leaching rate under inert atmosphere of nitrogen (other leaching parameters: agitation rate of  $100 \text{ r}\cdot\text{min}^{-1}$ , particle size of  $48\text{--}75 \mu\text{m}$ , acid concentration of 15 wt%, liquid-to-solid ratio of 4:1, oxygen flow rate of  $0.16 \text{ L}\cdot\text{min}^{-1}$ )

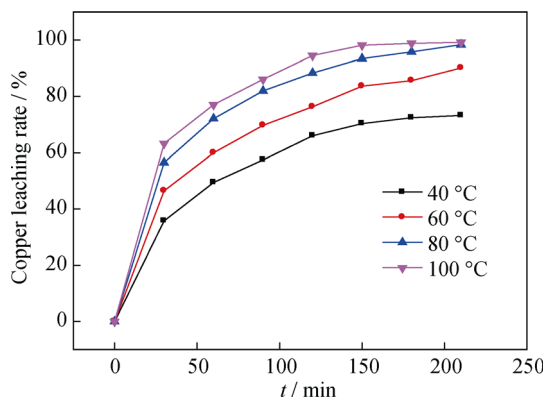
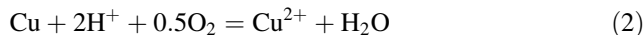


**Fig. 9** Effect of leaching temperatures on copper leaching rate deducted presence of CuO

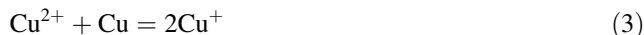
### 3.1.5 Catalytic effect of $\text{Cu}^{2+}$

It has been reported that copper tends to be corroded faster in the presence of cupric ions. The principle is believed to be as follows [24].

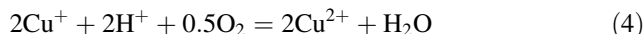
The cupric ions are extracted according to the following overall reaction.



Cuprous ions are generated by the reaction of cupric ions and copper [25–27].



Cuprous ions are then oxidized to copper ions by oxygen rapidly.



So Reaction (2) can be assumed to be the combination of Reactions (3) and (4). The intermediate of  $\text{Cu}^+$  is an ideal carrier of oxygen, which is considered to be a type of catalyst promoting the dissolving of copper. Hence, once a small amount of  $\text{Cu}^{2+}$  are generated, the copper dissolution rate will be accelerated by the catalytic effect of  $\text{Cu}^{2+}$  with the presence of  $\text{O}_2$ , which is thought to be autocatalytic reaction.

From the aforementioned results, it can be seen that it takes a relative long time to achieve the dissolving equilibrium state, about 3 h. In order to shorten the leaching time for copper, different amounts of  $\text{Cu}^{2+}$  were added into the initial sulfuric acid solution, ranging from 10 to  $30 \text{ g}\cdot\text{L}^{-1}$ . Under these conditions, the copper leaching results are shown in Fig. 10. Compared with that without adding  $\text{Cu}^{2+}$ , the leaching time could be shortened from 3.0 to 1.5 h when  $10 \text{ g}\cdot\text{L}^{-1} \text{ Cu}^{2+}$  was added and copper leaching rate of 99 % is guaranteed. Little difference is shown for different amounts of copper added. Consequently,  $\text{Cu}^{2+}$  should play the similar role that literatures mentioned [24–27], promoting the transfer of oxygen and accelerating the oxidative leaching of copper.

### 3.1.6 Catalytic effect of activated carbon

The effect of activated carbon on the copper leaching rate was assessed, and the amount of activated carbon added was ranging from 3 to  $8 \text{ g}\cdot\text{L}^{-1}$ . A plot of copper leaching rate over activated carbon concentration is presented in Fig. 11. It can be observed that the leaching rate of copper increases significantly with the addition of activated carbon to the solution, and more than 99 % copper could be leached out in 60 min when the concentration of activated carbon is more than  $5 \text{ g}\cdot\text{L}^{-1}$ . The optimum activated carbon concentration is then chosen to be  $5 \text{ g}\cdot\text{L}^{-1}$ .



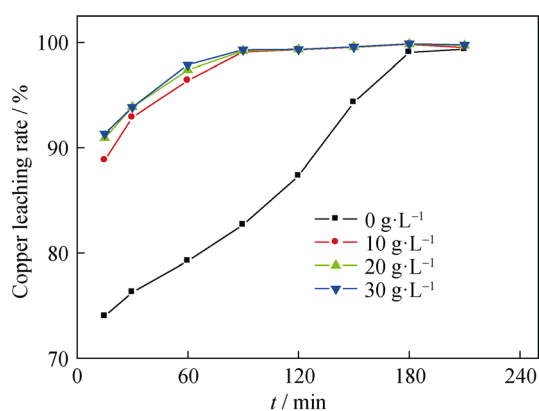


**Fig. 10** Effect of  $\text{Cu}^{2+}$  concentrations on copper leaching rate (other leaching parameters: agitation rate of  $100 \text{ r}\cdot\text{min}^{-1}$ , particle size of  $48\text{--}75 \mu\text{m}$ , acid concentration of  $15 \text{ wt}\%$ , liquid-to-solid ratio of  $4:1$ , temperature of  $80 \text{ }^\circ\text{C}$ , oxygen flow rate of  $0.16 \text{ L}\cdot\text{min}^{-1}$ )

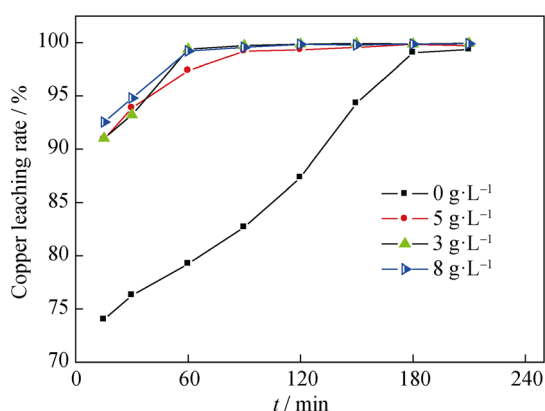


**Fig. 11** Effect of activated carbon concentrations on copper leaching rate (other leaching parameters: agitation rate of  $100 \text{ r}\cdot\text{min}^{-1}$ , particle size of  $48\text{--}75 \mu\text{m}$ , acid concentration of  $15 \text{ wt}\%$ , liquid-to-solid ratio of  $4:1$ , temperature of  $80 \text{ }^\circ\text{C}$ , oxygen flow rate of  $0.16 \text{ L}\cdot\text{min}^{-1}$ )

There are several types of oxygenic functional groups at the surface of activated carbon, including carboxyl, carboxyl anhydride, carbonyl, lactone, phenolic, ether, pyrone and chromene, etc., as shown in Fig. 12 [12, 28–32]. Surface oxygenic functional groups may directly react with Cu species, resulting in their oxidation, or in an indirect way through the reduction of oxygen to hydrogen peroxide [33]. Oxygenic groups such as chromene or quinone groups have lower redox potential than that of the  $\text{O}_2/\text{H}_2\text{O}_2$  pair ( $0.695 \text{ V}$ ) [33]. So activated carbon can generate hydrogen peroxide once in contact with molecular oxygen in acidic slurry [34, 35]. Because the  $\text{H}_2\text{O}_2/\text{H}_2\text{O}$  ( $1.763 \text{ V}$ ) pair is higher than the  $\text{O}_2/\text{H}_2\text{O}$  pair ( $1.229 \text{ V}$ ), the oxidation rate of Cu to  $\text{Cu}^{2+}$  (slope of copper leaching rate against time) is faster than that of the oxidative leaching without activated carbon. So the oxidative leaching with activated carbon takes about 90 min which is shorter than that

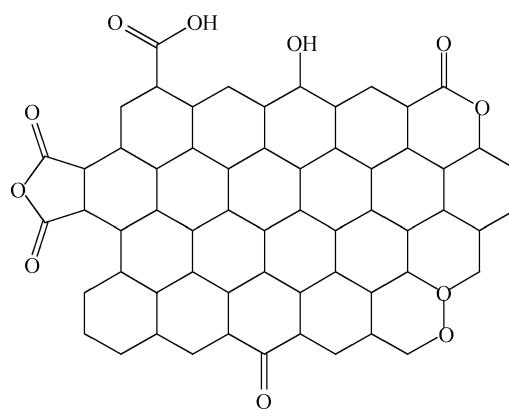


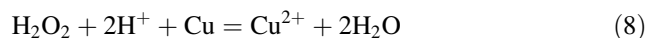
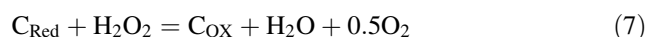
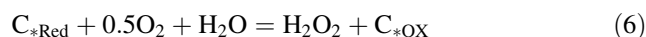
**Fig. 12** Some type of oxygen-containing functional groups in activated carbon

without activated carbon (around 180 min) for reaching the leaching rate of  $99 \%$ .

According to the above analysis, the possible mechanism might be described using the following equations,



where  $\text{C}_{\text{OX}}$  represents a surface functional group with oxidation–reduction potential higher than that of the  $\text{Cu}^{2+}/\text{Cu}$  pair. This group will be able to oxidize Cu to  $\text{Cu}^{2+}$ . Then, the reduced functional group is oxidized by oxygen and hydrogen peroxide ( $\text{H}_2\text{O}_2$ ) with strong oxidizing power will be generated, which will further promote the oxidization of the functional group and copper.



where  $\text{C}_{\text{OX}}$  represents a surface functional group with oxidation–reduction potential higher than that of the  $\text{Cu}^{2+}/\text{Cu}$  pair;  $\text{C}_{*\text{Red}}$  and  $\text{C}_{\text{Red}}$  represent the surface reduced functional group;  $\text{C}_{*\text{OX}}$  represents a surface oxidation group where the surface reduced functional group has been oxidized by  $\text{H}_2\text{O}_2$ . Hence, it is proposed that copper could be oxidized to  $\text{Cu}^{2+}$  species by  $\text{H}_2\text{O}_2$  generated from the reduction of molecular oxygen. In order to verify the existence of hydrogen peroxide in the reaction media, another experiment was carried out to test the solution in which oxygen had contacted with acidic slurry containing the activated carbon at  $80 \text{ }^\circ\text{C}$  for 30 min. Figure 13a shows the molecular absorption spectra measured with each of the obtained solutions. For the purpose of comparison, Fig. 13b shows the spectrum of a reference solution containing  $0.05 \text{ mol}\cdot\text{L}^{-1} \text{ H}_2\text{O}_2$ . The results in Fig. 13 jointly suggest that hydrogen peroxide is generated in acidic solution upon contacting between molecular oxygen and activated carbon.

Moreover, activated carbon is a type of porous material with large surface areas, which can have a strong adsorption

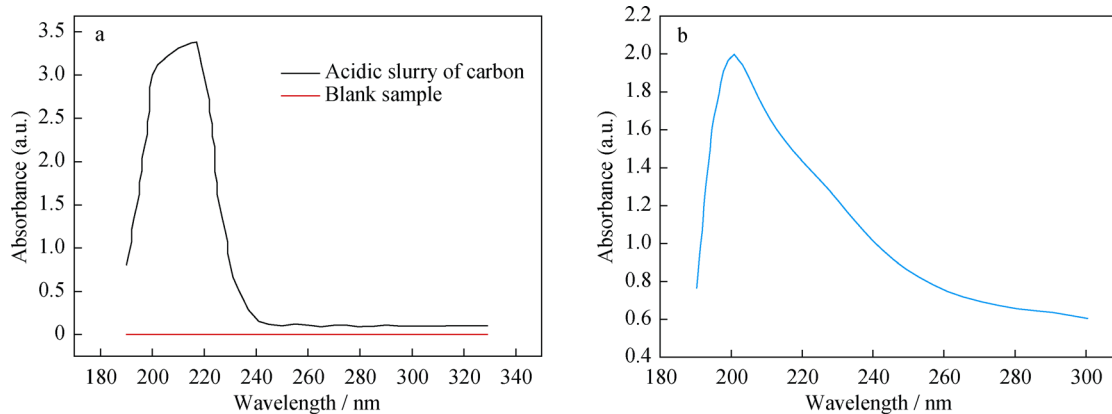


**Fig. 13** Molecular absorption spectra for **a** acid solutions with or without activated carbon in presence of O<sub>2</sub> and **b** a reference acid solution (15 wt% H<sub>2</sub>SO<sub>4</sub>) without activated carbon but with 0.05 mol·L<sup>-1</sup> H<sub>2</sub>O<sub>2</sub>

capability for Cu<sup>2+</sup>. Therefore, the real time concentration of Cu<sup>2+</sup> in the leachate will descend, which can thermodynamically accelerate the leaching. Thus, both of the two aspects would make contribution to the acceleration of copper dissolution from the copper–cadmium-bearing slag.

### 3.2 Kinetics analysis

Solid–fluid heterogeneous reactions are common in chemical and hydrometallurgical processes. In order to determine the macro-dynamic parameters and leaching rate controlling step for copper, the popular shrinking core model was utilized to fit the data [36]. In solid–fluid reaction systems, the reaction rate may be controlled by one (sometimes may more than one) of the following steps: the reactant diffusion through the fluid phase (external diffusion), the chemical reaction at the surface of the mineral (chemical reaction), or the reactant diffusion through the product layer (internal diffusion).

According to the shrinking core model, the relationships between the leaching rate of copper (*X*) and time (*t*) with different rate-determining steps can be described as [37]:

(1) External diffusion control

$$X = kt \tag{9}$$

where *X* is the fraction reacted, *k* is the reaction rate constant, and *t* is the reaction time.

(2) Internal diffusion control

$$1 + 2(1 - X) - 3(1 - X)^{2/3} = kt \tag{10}$$

(3) Chemical reaction control

$$1 - (1 - X)^{1/3} = kt \tag{11}$$

It can be seen that the controlling mode can be determined by the plot of left side of the equations against time (*t*) from Eqs. (9)–(11), which should be linear. Once the mode is selected, the slope of the fitted line is the reaction rate constant (*k*); meanwhile, the temperature dependence of *k* can be described by Arrhenius equation,

$$k = A \exp(-E_a/RT) \tag{12}$$

Or

$$k = \ln A - E_a/RT \tag{13}$$

where *A* is the frequency factor, *E<sub>a</sub>* is the apparent activation energy, *R* is gas constant, and *T* is temperature.

The three equations were used to fit the copper leaching rates at 80 °C with data from Fig. 9, as shown in Fig. 14. From the degree of linearity (*R* value), the internal diffusion control of shrinking core model is found to fit the leaching data better than the other two modes. Then the copper leaching rates at different temperatures versus

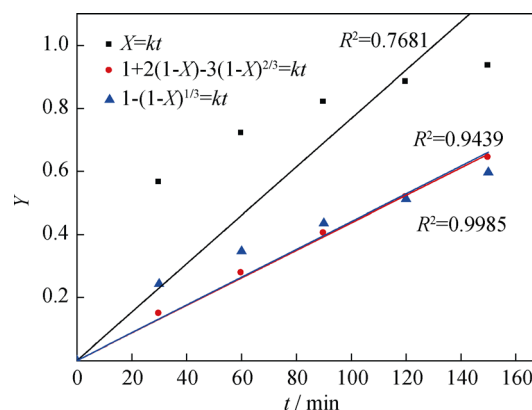


**Fig. 14** Comparison of linear fitting results of three modes for Cu leaching rates at 80 °C (*Y* = *X* or  $1 + 2(1 - X) - 3(1 - X)^{2/3}$  or  $1 - (1 - X)^{1/3}$ )

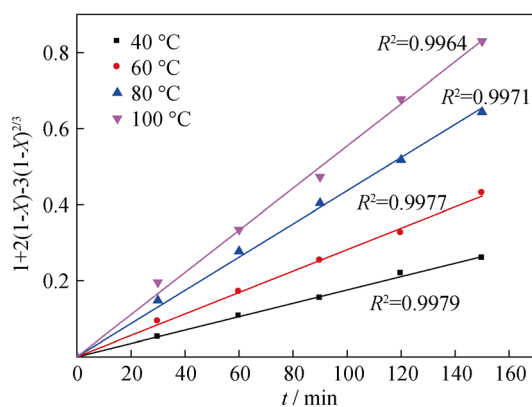


**Fig. 15** Relationships of  $1 + 2(1 - X) - 3(1 - X)^{2/3}$  with leaching time at various temperatures

**Table 2** Fitted values of reaction rate constant ( $k$ ) at various temperatures

$T/^\circ\text{C}$	40	60	80	100
$k$	0.0018	0.0028	0.0044	0.0055

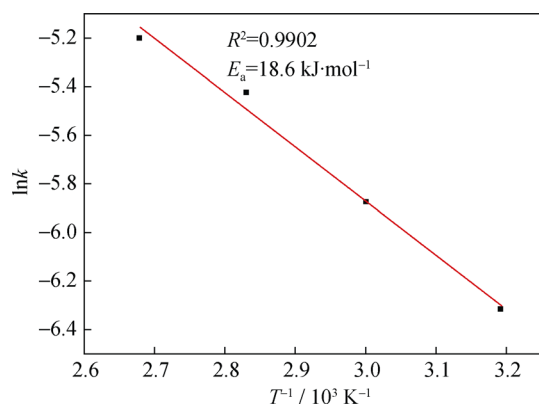


**Fig. 16** Arrhenius plot of reaction rate against reciprocal of temperature

leaching time were all fitted using Eq. (10), as given in Fig. 15. After linear regression, the slope for each fitted line is obtained, which is  $k$  value, as shown in Table 2.

**Table 3** Typical compositions of leachate and leaching residue

Nos.	Ion concentration/(g·L <sup>-1</sup> )			Residue composition/wt%				Residue rate/%	Leaching rate/%		
	Zn <sup>2+</sup>	Cu <sup>2+</sup>	Cd <sup>2+</sup>	Zn	Cu	Cd	Pb		Zn	Cu	Cd
1	55.06	18.76	36.84	0.11	0.63	1.53	16.68	3.70	99.99	99.78	99.75
2	55.20	18.28	40.22	0.41	1.60	1.46	11.30	4.30	99.92	99.23	99.67
3	56.18	18.47	40.30	0.39	0.61	1.20	10.34	4.20	99.92	99.68	99.70
Average	55.48	18.5	39.12	0.30	0.95	1.40	12.77	4.07	99.94	99.56	99.71

Then the Arrhenius plot by plotting the logarithm of  $k$  versus inverse temperature ( $1/T$ ) is obtained, as provided in Fig. 16. The resulting negative sloped line is useful for finding the missing parameter values of the Arrhenius equation. Extrapolation of the line back to the y-intercept yields the value for  $\ln A$ , and the slope of the line is equal to the negative apparent activation energy divided by the gas constant ( $R$ ). It is calculated that the apparent activation energy is  $18.6 \text{ kJ}\cdot\text{mol}^{-1}$ , which further evidences that copper leaching is controlled by diffusion, similar to the observations reported in literature for conventional leaching process [19].

### 3.3 Suggested treatment of leachate and leaching residue

Under the optimized leaching conditions, the leachate containing about  $55.48 \text{ g}\cdot\text{L}^{-1} \text{ Zn}^{2+}$ ,  $18.50 \text{ g}\cdot\text{L}^{-1} \text{ Cu}^{2+}$  and  $39.12 \text{ g}\cdot\text{L}^{-1} \text{ Cd}^{2+}$  with pH value of 2–4 could be obtained, as shown in Table 3. Taking advantage of the weak acid circumstance, these metals can be extracted separately and directly by selective reduction through the controlling of reductant dosage. Copper and zinc ions can also be separated by solvent extraction using LIX984 and di-(2-ethyl-hexyl) phosphate acid (D2EHPA), respectively [38]. And LIX841 is another type of extractant [39]. Abundant of

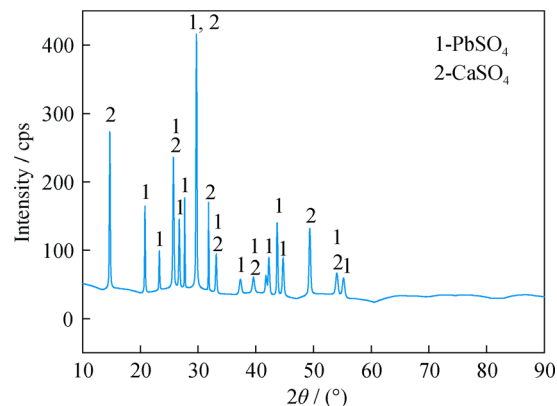
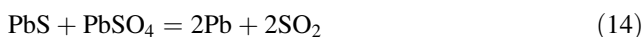


**Fig. 17** XRD pattern of leaching residue



researches have been focused on this issue, which is not a knotty problem [40–44].

For the leaching residue, the yield is about 4 wt% of original copper–cadmium-bearing slag. The phase composition was analyzed by XRD, as shown in Fig. 17. The result indicates that the phases are mainly  $\text{PbSO}_4$  and  $\text{CaSO}_4$ . And the chemical composition analysis result shows that about 13 % Pb is contained in the residue, which can be recycled by Pb smelting technology in an Isa furnace. The way is that the Pb-containing concentrate and the  $\text{PbSO}_4$ -containing leaching residue can be mixed and placed in the furnace, and the reaction of these two will form Pb metal through the following reaction [45].



#### 4 Conclusion

The oxidative leaching behavior of copper–cadmium-bearing slag produced from zinc hydrometallurgical process in sulfuric acid solution was investigated. The results show that the slag could be easily leached and a pretty high leaching rate of more than 99 % is reached under the conditions of temperature of 80 °C, sulfuric acid concentration of 15 wt%, liquid-to-solid ratio of 4:1, leaching time of 3 h, oxygen flow rate of 0.16 L·min<sup>-1</sup>, and stirring speed of 100 r·min<sup>-1</sup>. However, if some catalysts, such as  $\text{Cu}^{2+}$ , activated carbon, were introduced into the slurry, the leaching speed for copper would be accelerated dramatically, and the leaching time could be shortened from 3.0 to 1.5 or 1.0 h. The action mechanism of these types of catalysts should be the same to some extent, which are performed as the oxygen carrier, changing the direct oxidation of copper by  $\text{O}_2$  to indirect oxidation by the formed intermediate. The leaching dynamic fitting results reveal that the apparent activation energy for copper leaching is 18.6 kJ·mol<sup>-1</sup>, and it is controlled by internal diffusion.

For the typical leachate and leaching residue, suggested dealing methods were provided. The valuable metal ions in the leachate can be recycled separately by selective reduction or solvent extraction. The Pb component in the residue can be further treated by pyro-metallurgical Pb smelting technology.

**Acknowledgments** This work was financially supported by the National Science & Technology Pillar Program during the Twelfth Five-Year Plan Period of China (No. 2012BAC12B01) and the Major Scientific and Technological Special Project of Hunan Province, China (No. 2012FJ1010).

#### References

- [1] Kim T, Senanayake G, Kang J, Sohn J, Rhee K, Lee S, Shin S. Reductive acid leaching of spent zinc–carbon batteries and

- oxidative precipitation of Mn–Zn ferrite nanoparticles. *Hydrometallurgy*. 2009;96(1):154.
- [2] Babu MN, Sahu K, Pandey B. Zinc recovery from sphalerite concentrate by direct oxidative leaching with ammonium, sodium and potassium persulphates. *Hydrometallurgy*. 2002; 64(2):119.
- [3] Li B, Pan DA, Jiang YH, Tian JJ, Zhang SG, Zhang K. Recovery of copper and tin from stripping tin solution by electrodeposition. *Rare Met*. 2014;33(3):353.
- [4] de Souza AD, Pina PS, Leão VA. Bioleaching and chemical leaching as an integrated process in the zinc industry. *Miner Eng*. 2007;20(6):591.
- [5] Wang MY, Wang XW, Jiang CJ, Tao CF. Solvent extraction of molybdenum from acidic leach solution of Ni–Mo ore. *Rare Met*. 2014;33(1):107.
- [6] Ibarra-Galvan V, López-Valdivieso A, Tong X, Cui YQ. Role of oxygen and ammonium ions in silver leaching with thiosulfate–ammonia–cupric ions. *Rare Met*. 2013;33(2):225.
- [7] Shao Q, Du X, Wang L, Lan RZ. Present status of reutilization of copper–cadmium slag. *Chin J Hydrometall*. 2003;22(2):66.
- [8] Ning Q. Study on the recovery of zinc, cadmium, copper from copper–cadmium slag. *Chin J Hydrometall*. 1998;1:41.
- [9] Kasprzyk-Hordern B, Ziólek M, Nawrocki J. Catalytic ozonation and methods of enhancing molecular ozone reactions in water treatment. *Appl Catal-B Environ*. 2003;46(4):639.
- [10] Rivera-Utrilla J, Sánchez-Polo M, Gómez-Serrano V, Álvarez PM, Alvim-Ferraz MCM, Dias JM. Activated carbon modifications to enhance its water treatment applications. An overview. *J Hazard Mater*. 2011;187(1–3):1.
- [11] Stoekli HF, Rebstein P, Ballerini L. On the assessment of microporosity in active carbons, a comparison of theoretical and experimental data. *Carbon*. 1990;28(6):907.
- [12] Rodríguez-reinoso F. The role of carbon materials in heterogeneous catalysis. *Carbon*. 1998;36(3):159.
- [13] Laine J, Severino F, Labady M. Optimum Ni composition in sulfided Ni–Mo hydrodesulfurization catalysts: effect of the support. *J Catal*. 1994;147(1):355.
- [14] Laine J, Labady M, Severino F, Yunes S. Sink effect in activated carbon-supported hydrodesulfurization catalysts. *J Catal*. 1997; 166(2):384.
- [15] Nunez C, Viñals J. Kinetics of leaching of zinc ferrite in aqueous hydrochloric acid solutions. *Metall Mater Trans B*. 1984;15(2):221.
- [16] Elgersma F, Kamst G, Witkamp G, van Rosmalen G. Acidic dissolution of zinc ferrite. *Hydrometallurgy*. 1992;29(1):173.
- [17] Elgersma F, Witkamp GJ, van Rosmalen GM. Kinetics and mechanism of reductive dissolution of zinc ferrite in  $\text{H}_2\text{O}$  and  $\text{D}_2\text{O}$ . *Hydrometallurgy*. 1993;33(1–2):165.
- [18] Langová Š, Leško J, Matýsek D. Selective leaching of zinc from zinc ferrite with hydrochloric acid. *Hydrometallurgy*. 2009; 95(3):179.
- [19] Bobeck GE, Su H. The kinetics of dissolution of sphalerite in ferric chloride solution. *Metall Mater Trans B*. 1985;16(3):413.
- [20] Zhang Y, Li X, Pan L, Liang X, Li X. Studies on the kinetics of zinc and indium extraction from indium-bearing zinc ferrite. *Hydrometallurgy*. 2010;100(3):172.
- [21] Kim J, Kaurich TA, Sylvester P, Gonzalez-Martin A. Enhanced selective leaching of chromium from radioactive sludges. *Sep Sci Technol*. 2006;41(1):179.
- [22] Dutrizac J. The leaching of sulphide minerals in chloride media. *Hydrometallurgy*. 1992;29(1):1.
- [23] Aydogan S, Aras A, Canbazoglu M. Dissolution kinetics of sphalerite in acidic ferric chloride leaching. *Chem Eng J*. 2005; 114(1):67.
- [24] Tindall G, Bruckenstein S. Determination of heterogeneous equilibrium constants by chemical stripping at a ring-disk electrode. Evaluation of the equilibrium constant for the reaction

- copper + copper(II)  $\rightarrow$  2copper(I) in 0.2 M sulfuric acid. *Anal Chem.* 1968;40(10):1402.
- [25] Mokmeli M, Wassink B, Dreisinger D. Equilibrium cuprous concentrations in copper sulfate–sulfuric acid solutions containing 50–110 g/L  $\text{Cu}^{2+}$  and 10–200 g/L  $\text{H}_2\text{SO}_4$  at 50–95°C. *Hydrometallurgy.* 2012;2012(121–124):100.
- [26] Ciavatta L, Ferri D, Palombari R. On the equilibrium  $\text{Cu}^{2+} + \text{Cu(s)} \rightleftharpoons 2\text{Cu}^+$ . *J Inorg Nucl Chem.* 1980;42(4):593.
- [27] Desmarquest JP, Trinh-Dinh C, Bloch O. Determination of normal electrochemical potentials of redox couples reducers  $\text{Cu}^{2+}/\text{Cu}^+$  and  $\text{Cu}^+/\text{Cu}^0$  in methanol. *J Inorg Nucl Chem.* 1970;27(1):101.
- [28] Radovic LR. *Chemistry and Physics of Carbon.* New York: CRC Press; 2000. 121.
- [29] Rodriguez-Reinoso F, Molina-Sabio M. Textural and chemical characterization of microporous carbons. *Adv Colloid Interface.* 1998;76:271.
- [30] Randin J-P, Yeager E. Differential capacitance study on the edge orientation of pyrolytic graphite and glassy carbon electrodes. *J Electroanal Chem.* 1975;58(2):313.
- [31] Derbyshire F, De Beer V, Abotsi G, Scaroni A, Solar J, Skrovanek D. The influence of surface functionality on the activity of carbon-supported catalysts. *Appl Catal.* 1986;27(1):117.
- [32] Boehm H. Some aspects of the surface chemistry of carbon blacks and other carbons. *Carbon.* 1994;32(5):759.
- [33] Hossain M, Tryk D, Yeager E. The electrochemistry of graphite and modified graphite surfaces: the reduction of  $\text{O}_2$ . *Electrochim Acta.* 1989;34(12):1733.
- [34] Tatsumi H, Nakase H, Kano K, Ikeda T. Mechanistic study of the autoxidation of reduced flavin and quinone compounds. *J Electroanal Chem.* 1998;443(2):236.
- [35] Ossowski T, Pipka P, Liwo A, Jeziorek D. Electrochemical and UV-spectrophotometric study of oxygen and superoxide anion radical interaction with anthraquinone derivatives and their radical anions. *Electrochim Acta.* 2000;45(21):3581.
- [36] He S, Wang J, Yan J. Pressure leaching of synthetic zinc silicate in sulfuric acid medium. *Hydrometallurgy.* 2011;108(3):171.
- [37] Ryczaj K, Riesenkauf W. Kinetics of the dissolution of zinc-magnesium ferrites in sulphuric acid solutions related to zinc leach processes. *Hydrometallurgy.* 1983;11(3):363.
- [38] Lan ZY, Hu YH, Liu JS, Wang J. Solvent extraction of copper and zinc from bioleaching solutions with LIX984 and D2EHPA. *J Cent South Univ Technol.* 2005;12(1):45.
- [39] Reddy BR, Priya DN. Process development for the separation of copper(II), nickel(II) and zinc(II) from sulphate solutions by solvent extraction using LIX 84 I. *Sep Purif Technol.* 2005;45(2):163.
- [40] Owusu G. Selective extraction of copper from acidic zinc sulfate leach solution using LIX 622. *Hydrometallurgy.* 1999;51(1):1.
- [41] Gupta B, Deep A, Malik P. Extraction and recovery of cadmium using Cyanex 923. *Hydrometallurgy.* 2001;61(1):65.
- [42] Gouvea LR, Morais CA. Recovery of zinc and cadmium from industrial waste by leaching/cementation. *Miner Eng.* 2007;20(9):956.
- [43] Mellah A, Benachour D. The solvent extraction of zinc and cadmium from phosphoric acid solution by di-2-ethylhexyl phosphoric acid in kerosene diluent. *Chem Eng Process.* 2006;45(8):684.
- [44] Pereira DD, Rocha SDF, Mansur MB. Recovery of zinc sulphate from industrial effluents by liquid–liquid extraction using D2EHPA (di-2-ethylhexyl phosphoric acid). *Sep Purif Technol.* 2007;53(1):89.
- [45] He S, Wang J, Yan J. Pressure leaching of high silica Pb–Zn oxide ore in sulfuric acid medium. *Hydrometallurgy.* 2010;104(2):235.